Dalton Transactions

Accepted Manuscript

ROYAL SOCIETY OF CHEMISTRY

www.rsc.org/dalton

Magnetic and luminescent properties of lanthanide coordination polymers with asymmetric biphenyl-3,2′,5′-tricarboxylate

Jie Zhao,[a] Guan-Hong Zhu,[a] Li-Qiong Xie,[a] Ye-Si Wu,[a] Hai-Lun Wu,[a] Ai-Ju Zhou,[a] Zun-Yuan Wu,[a] Jing Wang*[a], Yan-Cong Chen[b] and Ming-Liang Tong[b]

An asymmetric ligand was employed to construct eight (3,6)-connected lanthanide complexes exhibiting slow magnetization relaxation behaviour and characteristic luminescent properties.

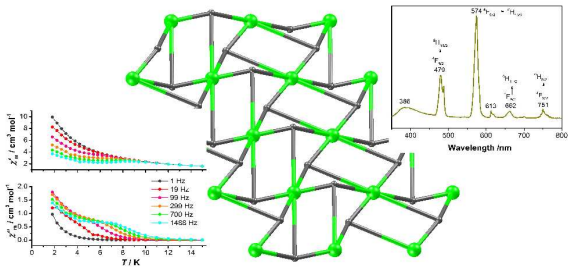

Cite this: DOI: 10.1039/c0xx00000x

www.rsc.org/xxxxxx

ARTICLE TYPE

Magnetic and luminescent properties of lanthanide coordination polymers with asymmetric biphenyl-3,2′,5′-tricarboxylate

Jie Zhao,[a] Guan-Hong Zhu,[a] Li-Qiong Xie,[a] Ye-Si Wu,[a] Hai-Lun Wu,[a] Ai-Ju Zhou,[a] Zun-Yuan Wu,[a] Jing Wang*[a], Yan-Cong Chen[b] and Ming-Liang Tong[b]

Received (in XXX, XXX) Xth XXXXXXXXX 20XX, Accepted Xth XXXXXXXXX 20XX
DOI: 10.1039/b000000x

Eight isostructural lanthanide coordination polymers $[Ln(bptc)(phen)(H_2O)]_n$ (Ln = Dy for 1, Eu for 2, Tb for 3, Gd for 4, Sm for 5, Nd for 6, Yb for 7, Pr for 8) were successfully prepared based on bridging asymmetric polycarboxylate ligand biphenyl-3,2′,5′-tricarboxylic acid (H_3bptc) and chelating 1,10-phenanthroline (phen) coligand. Single crystal X-ray analysis reveals that complexes 1-8 have a (3,6)-connected CdI_2-type coordination network consisting of paddle-wheel dimers $[Ln_2(CO_2)_4]$. The magnetic and fluorescent properties of 1-8 have been investigated. Significantly, the Dy(III) complex 1 behaves with slow relaxation of the magnetization, where the frequency-dependent out-of-phase signals are noticed.

Introduction

The exciting area of coordination chemistry for lanthanide ions has become an attractive field of research with almost unlimited perspectives.[1] The lanthanide coordination polymers with fascinating structures and new topologies have potential applications in catalysis, medicine and material science, thanks to their intriguing spectroscopic and magnetic properties.[2] Most trivalent lanthanide ions can exhibit narrow and characteristic emission in the visible to near-infrared part of the optical spectrum, due to internal 4f–4f transitions. However, the direct excitation of the metals is very inefficient, due to the weak light absorption for the forbidden f-f transitions. Upon incorporation into coordination polymers, suitable organic ligands can enhance the optical absorption, followed by energy transfer to the lanthanide ions, known as "luminescence sensitization" or "antenna effect".[3,4] Apart from the excellent photophysical properties, the magnetic properties of lanthanide coordination polymers are uncommon due to the presence of strong unquenched orbital angular momentum originating from f electrons that are shielded by s and p electrons.[5] Following the conspicuous discovery of single-molecule magnets, researchers have rivaled to find adequate systems displaying this property. Dysprosium with large intrinsic magnetic anisotropy was targeted as the favored Ln(III) ion and its coordination polymers have attracted more interest in the field of molecular magnetism.[6] Lanthanide-based single-molecule magnets (SMMs) and single-ion magnets (SIMs) exhibit slow relaxation of the magnetization at low temperature, providing the promising candidates to make spintronic devices.[7]

More and more efforts for lanthanide coordination polymers have mainly focused on the construction and preparation of versatile coordination polymers, as well as the structure–property relationships. Comparably, the large ionic radius of lanthanide ions results in high and variable coordination numbers, which may cause difficulty in controlling the synthetic reaction than transition-metal ones.[8] Among the strategies, the rational selection of organic ligands or coligands according to their length, rigidity and functional groups is important for the assembly of structural controllable lanthanide coordination polymers. As is well-known, lanthanide ions have high affinity for hard donor atoms and ligands containing oxygen or hybrid oxygen−nitrogen atoms, especially multicarboxylate ligands. Of the aromatic carboxylates, the rigid 1,3,5-benzenetricarboxylate,[9] 1,2,4,5-benzenetetracarboxylate,[10] 1,2,3,4,5-benzenepentacarboxylate[11] and 1,2,3,4,5,6-benzenehexacarboxylate[12] have been extensively studied. Comparably, the biphenyl ligands possess more flexibility because of the free rotation of the C-C bond between the phenyl rings and therefore may result in more diverse structures. More recently, versatile coordination polymers assembled from biphenyl carboxylate ligands, such as biphenyldicarboxylate,[13] biphenyl-3,4′,5-tricarboxylate,[14] and biphenyl-3,5,3′,5′/3,4,3′,4′/2,4,2′,4′-tetracarboxylate[15] compounds have been reported. Most of these polycarboxylate ligands possess highly symmetric geometry which are suitable to result symmetric networks. In contrast, coordination polymers based on asymmetric polycarboxylate ligands are far less prevalent, probably due to the asymmetric geometry making it difficult to predict the final coordination networks, especially the lanthanide ones.[16]

As one type of bridging biphenyl polycarboxylate ligand, biphenyl-3,2′,5′-tricarboxylic acid (H_3bptc) with rotatable coordination vertex and asymmetric geometry has been rarely documented to construct coordination polymers.[17] By investigation on H_3bptc, we have obtained four complexes with magnetic and fluorescent properties and discussed the conformations' stability and coordination modes of the ligand by theoretical calculation. Wang and co-workers reported one cobalt-bptc complex exhibiting slow magnetic relaxation behaviour, but the lanthanide complexes have been unexplored up to now. As a continuation of our previous investigation on the

asymmetric H_3bptc ligand, we present here a family of lanthanide complexes $[Ln(bptc)(phen)(H_2O)]_n$ (Ln = Dy for **1**, Eu for **2**, Tb for **3**, Gd for **4**, Sm for **5**, Nd for **6,** Yb for **7,** Pr for **8,** phen = 1,10-phenanthroline), which exhibit the isostructural 2-D coordination network consisting of paddle-wheel dimers $[Ln_2(CO_2)_4]$. The magnetic and fluorescent properties have been investigated.

Experimental section

Materials and methods

The reagents and solvents employed were commercially available and used as received without further purification. The C, H, and N microanalyses for the eight complexes were performed on fresh samples, with Elementar Vario-EL CHN elemental analyzer. FT-IR spectra were recorded from KBr pellets in the range of 4000-400 cm^{-1} on a Bio-Rad FTS-7 spectrometer. X-ray powder diffraction (XRPD) intensities for the eight complexes were measured at 293 K on a Bruker D8 X-ray diffratometer (Cu-Kα, λ = 1.54056 Å). The crushed poly-crystalline powder samples were prepared by crushing the crystals and scanned from 5-60^o with a step of 0.1^o/s, and calculated patterns were generated with PowderCell. Thermogravimetric (TG) analyses were carried out on NETZSCH TG209F3 thermogravimetric analyzer. Variable-temperature magnetic susceptibility measurements were performed on a SQUID magnetometer MPMS (Quantum Design) at 1.0 kOe for **1**-**4** and the diamagnetic correction was applied from Pascal's constants. The emission/excitation spectra for **1**-**3** and **5**-**7** were measured on an FLS-980 Fluorescence Spectrophotometer.

Preparation of complexes 1−8.

A mixture of 3,2′,5′-H_3bptc (0.053g, 0.20 mmol) and phen (0.036 g, 0.20 mmol) in H_2O (5.0 mL) were added to an aqueous solution (12.0 mL) of $LnCl_3{\cdot}6H_2O$ ($DyCl_3{\cdot}6H_2O$ for **1**, 0.079 g, 0.20 mmol; $EuCl_3{\cdot}6H_2O$ for **2**, 0.073 g, 0.20 mmol; $TbCl_3{\cdot}6H_2O$ for **3**, 0.075 g, 0.20 mmol; $Gd(NO_3)_3{\cdot}6H_2O$ for **4**, 0.087 g, 0.20 mmol; $SmCl_3{\cdot}6H_2O$ for **5**, 0.073 g, 0.20 mmol; $NdCl_3{\cdot}6H_2O$ for **6**, 0.072 g, 0.20 mmol; $YbCl_3{\cdot}6H_2O$ for **7**, 0.073 g, 0.20 mmol; $PrCl_3{\cdot}6H_2O$ for **8**, 0.073 g, 0.20 mmol) and stirred. After stirring for 20 min in air, the mixture was placed into a 25 mL Teflon-lined autoclave under autogenous pressure heated at 160 °C for 72 h, and then the autoclave was cooled over a period of 24 h at a rate 5 °C·h^{-1}. After filtration, the products were washed with distilled water and then dried, colorless crystals of **1-8** were obtained suitable for X-ray diffraction analysis.

For **1**: Yield ca. 75% based on Dy. IR (KBr, cm^{-1}): 3621m, 3057m, 1652vs, 1583s, 1560s, 1399vs, 1261m, 1145w, 1099w, 1042w, 846m, 765m, 719m, 569m, 489w, 431w. Elemental analysis Calcd (%) for $C_{27}H_{17}N_2O_7Dy$: C, 50.36; H, 2.66; N, 4.35. Found: C, 50.49; H, 2.54; N, 4.22.

For **2**: Yield ca. 85% based on Eu. IR (KBr, cm^{-1}): 3610m, 3057m, 1641vs, 1583s, 1399vs, 1261m, 1145w,1099w, 846m,754m, 731m, 558m, 501w, 420w. Elemental analysis Calcd (%) for $C_{27}H_{17}N_2O_7Eu$: C, 51.20; H, 2.71; N, 4.42. Found: C, 50.93; H, 2.79; N, 4.34.

For **3**: Yield ca. 78% based on Tb. IR (KBr, cm^{-1}): 3621m, 3057m, 1652vs, 1584s, 1387vs, 1272m, 1145w, 1099w, 858s, 731s, 559s, 489w, 420w. Elemental analysis Calcd (%) for $C_{27}H_{17}N_2O_7Tb$: C, 50.64; H, 2,68; N, 4,37. Found: C, 49.18; H, 2.66; N, 3.99.

For **4**: Yield ca. 72% based on Gd. IR (KBr, cm^{-1}): 3615m, 3462w, 3060m, 1636s, 1587s, 1555s, 1386vs, 1266m, 1145m, 1105m, 1040m, 960w, 839m, 815m, 767m, 718m, 703m, 557m, 485m, 421m. Elemental analysis Calcd (%) for $C_{27}H_{17}N_2O_7Gd$: C, 50.60; H, 2.65; N, 4.37. Found: C, 50.85; H, 2.72; N, 4.31.

For **5**: Yield ca. 80% based on Sm. IR (KBr, cm^{-1}): 3632m, 3057m, 1641vs, 1571vs, 1387vs, 1271m, 1157w, 1134m, 1099w, 1066w, 846m, 732m, 559m, 489w, 420w. Elemental analysis Calcd (%) for $C_{27}H_{17}N_2O_7Sm$: C, 51.33; H, 2.71; N, 4.43. Found: C, 51.18; H,2.79; N, 4.57.

For **6**: Yield ca. 68% based on Nd. IR (KBr, cm^{-1}): 3621m, 3426m, 3057m, 1630vs, 1583s, 1399vs, 1261m, 1145w, 1099w, 846m, 754m, 719m, 558m, 489w, 420w. Elemental analysis Calcd (%) for $C_{27}H_{17}N_2O_7Nd$: C, 51.83; H, 2.74; N, 4.48. Found: C, 51.73; H, 2.59; N, 4.54.

For **7**: Yield ca. 52% based on Yb. IR (KBr, cm^{-1}): 3615m, 3044m, 1652s, 1587s, 1540s, 1395s, 1257m, 1145m, 1105m, 1048m, 960w, 840m, 815m, 758m, 727m, 703m, 557m, 485m, 421m. Elemental analysis Calcd (%) for $C_{27}H_{17}N_2O_7Yb$: C, 49.51; H, 2.60; N, 4.28. Found: C, 50.02; H, 2.59; N, 4.35.

For **8**: Yield ca. 90% based on Pr. IR (KBr, cm^{-1}): 3615m, 3060m, 1636s, 1587s, 1548s, 1386s, 1265m, 1137m, 1105m, 1048m, 960w, 847m, 815m, 767m, 727m, 703m, 558m, 485m, 421m. Elemental analysis Calcd (%) for $C_{27}H_{17}N_2O_7Pr$: C, 52.06; H, 2.73; N, 4.50. Found: C, 52.33; H, 2.62; N, 4.54.

Single-crystal structure determination

The data collection and structural analysis of crystals **1–8** were performed on a SMART (Bruker, 2002) diffractometer equipped with Mo-Kα radiation (λ= 0.71073 Å) at 296(2) K. Absorption corrections were applied by using multi-scan program SADABS. The structure was solved with direct methods and refined with a full-matrix least-squares technique with the SHELXTL program package.[18] Anisotropic thermal parameters were applied to all non-hydrogen atoms. The organic hydrogen atoms were generated geometrically (C-H 0.96 Å), the water hydrogen atoms were located from difference maps and refined with isotropic temperature factors. Crystal data as well as details of data collection and refinements are summarized in Table 1. Selected bond lengths and bond angles are listed in Table S1. Crystallographic data for the structures reported in this paper have been deposited in the Cambridge Crystallographic Data Center with CCDC reference numbers for complexes **1-8**.

Table 1 Crystallographic data and refinement parameters for complexes **1-5**.

Complex	**1**	**2**	**3**	**4**	**5**	**6**	**7**	**8**
Empirical formula	$C_{27}H_{17}N_2O_7Dy$	$C_{27}H_{17}N_2O_7Eu$	$C_{27}H_{17}N_2O_7Tb$	$C_{27}H_{17}N_2O_7Gd$	$C_{27}H_{17}N_2O_7Sm$	$C_{27}H_{17}N_2O_7Nd$	$C_{27}H_{17}N_2O_7Yb$	$C_{27}H_{17}N_2O_7Pr$
Fw	643.93	633.39	640.35	638.68	631.78	625.67	654.47	622.34

Crystal system	monoclinic	monoclinic	monoclinic	monoclinic	monoclinic	monoclinic	monoclinic	monoclinic
Space group	*C*2/*c*	*C*2/*c*	*C*2/*c*	*C*2/*c*	*C*2/*c*	*C*2/*c*	*C*2/*c*	*C*2/*c*
a (Å)	26.4924(4)	26.5642(9)	26.4871(9)	26.5096(14)	26.5873(4)	26.6409(13)	26.4030(13)	26.6602(8)
b(Å)	7.91130(10)	7.9347(3)	7.9190(3)	7.9323(5)	7.93790(10)	7.9552(4)	7.8892(4)	7.9699(2)
c (Å)	22.9666(3)	23.0722(7)	23.0086(8)	23.0546(12)	23.1031(3)	23.1863(12)	22.8578(11)	23.2273(7)
α (°)	90	90	90	90	90	90	90	90
β (°)	107.398(1)	107.415(2)	107.309(2)	107.419(3)	107.384(1)	107.432(3)	107.410(3)	107.4650(10)
γ (°)	90	90	90	90	90	90	90.00	90
V (Å^3)	4593.34(11)	4640.2(3)	4607.5(3)	4625.6(5)	4653.14(11)	4688.3(4)	4543.1(4)	4707.8(2)
Z	8	8	8	8	8	8	8	8
D_c (g cm^{-3})	1.862	1.813	1.846	1.834	1.804	1.773	1.914	1.756
μ (mm^{-1})	3.307	2.756	3.123	2.921	2.577	2.267	4.171	2.122
F(000)	2520	2496	2512	2504	2488	2472	2552	2464
Reflections collected	32489	17991	17907	18474	18778	17565	16941	17222
R_{int}	0.0388	0.0439	0.0281	0.0381	0.0285	0.0598	0.0511	0.0472
Gof	1.047	1.029	1.049	1.007	1.008	1.003	0.993	1.082
Final *R* indices	$R_1{}^a$ = 0.0216	$R_1{}^a$ = 0.0280	$R_1{}^a$ = 0.0246	$R_1{}^a$ = 0.0335	$R_1{}^a$ = 0.0245	$R_1{}^a$ = 0.0361	$R_1{}^a$ = 0.0299	$R_1{}^a$ = 0.0335
[$I > 2\sigma(I)$]	$wR_2{}^b$ = 0.0443	$wR_2{}^b$ = 0.0562	$wR_2{}^b$ = 0.0524	$wR_2{}^b$ = 0.0570	$wR_2{}^b$ = 0.0503	$wR_2{}^b$ = 0.0614	$wR_2{}^b$ = 0.0610	$wR_2{}^b$= 0.0827
R indices (all	$R_1{}^a$ = 0.0289	$R_1{}^a$ = 0.0404	$R_1{}^a$ = 0.0328	$R_1{}^a$ = 0.0566	$R_1{}^a$ = 0.0328	$R_1{}^a$ = 0.0606	$R_1{}^a$ = 0.0430	$R_1{}^a$ = 0.0525
data)	$wR_2{}^b$ = 0.0468	$wR_2{}^b$ = 0.0609	$wR_2{}^b$ = 0.0555	$wR_2{}^b$ = 0.0630	$wR_2{}^b$ = 0.0541	$wR_2{}^b$ = 0.0692	$wR_2{}^b$ = 0.0660	$wR_2{}^b$= 0.0912
CCDC number	1042943	1042932	1042930	1401554	1042931	1042933	1400605	1400604

$^a R_1 = \sum||F_o|-|F_c||/\sum|F_o|$, $^b wR_2 = [\sum w(F_o^2-F_c^2)^2/\sum w(F_o^2)^2]^{1/2}$

Results and discussion

Synthesis and X-ray crystal structures

According to our previous studies on flexible ligands in coordination polymers, the size and versatile coordination environments of the metal ions as well as the auxiliary ligands may play an important role in controlling the conformation of the flexible ligands.[19] In our latest research on the asymmetric biphenyl-3,2′,5′-tricarboxylic acid, the dihedral angle between two phenyl rings ranges from 35.4º to 56.6º by the rotation of the C-C bond between two phenyl rings in different coordination polymers (Fig. 1a). Herein, eight complexes are synthesized under hydrothermal condition by the reaction of lanthanide ions Dy(III) , Eu(III), Tb(III), Gd(III), Sm(III), Nd(III), Yb(III), Pr(III) with H_3bptc and phen ligands. The fully deprotonated bptc^{3-} ligand in the complexes adopts μ_5:η^2,η^2,η^1 bridging mode (Fig. 1b) and has a dihedral angle of 47.5º between two phenyl rings, similar to the reported complex $\{[Mn_3(bptc)_2(4,4'\text{-bpy})_3(H_2O)_2]\}_n$.[17a]

X-ray crystallographic study reveals that complexes **1**-**8** are isostructural (Table 1) except for the distinction of the lanthanide ion and crystallization in the monoclinic *C*2/*c* space group. As an example, the structure of the complex **1** will be described in detail. The asymmetric unit of $[Dy(bptc)(phen)(H_2O)]_n$ (**1**) contains one crystallographically independent Dy(III) atom, one deprotonated bptc^{3-}, one phen ligand and one coordinated water molecule (Fig. 2a). Each Dy(III) adopts a distorted square-antiprism geometry, coordinating to five carboxylate oxygen atoms (O1, O2B, O3C, O5A, O6D) from five bptc^{3-}, one water oxygen atom (O1W), and two nitrogen atoms (N1, N2) from one phen ligand. As shown in Fig. 2b and Table S1, the coplanar atoms O1, O2B, O5A, O6D with bond lengths of Dy-O(carboxylate) in the range 2.283(2)-2.3556(18) Å build up the square bottom plane. The top O3C, O1W, N1, N2 with bond length Dy-O(carboxylate) 2.3315(18) Å, Dy-O(water) 2.430(2) Å, Dy-N 2.553(3) and 2.575(3) Å are non-coplanar with a dihedral angle 16.0º, resulting in the distortion geometry. The bptc^{3-} ligand with a dihedral angle 47.5º of two phenyl rings is fully deprotonated. The three deprotonated carboxylate groups have different coordination modes including monodentate and bridging μ_2-η^1:η^1, to link five Dy(III) atoms (Fig. 1b). Four bridging carboxylate groups from distinctive ligands bind two Dy(III) atoms into a classic paddle-wheel dimer $[Dy_2(CO_2)_4]$ unit (Fig. 2b). Each dimer connects six bptc^{3-} ligands, while each bptc^{3-} ligand connecting three dimers. In the dimeric unit, the Dy···Dy distance is 4.3 Å, compared to the reported structures.[20] As shown in Fig. 2c, the different connecting of bptc^{3-} ligands leads to two interunit Dy_2···Dy_2 distances of 7.9 Å and 12.1 Å forming a parallelogram (Fig. 2c). The dimeric units are connected by bptc^{3-} ligands to generate a 2-D coordination

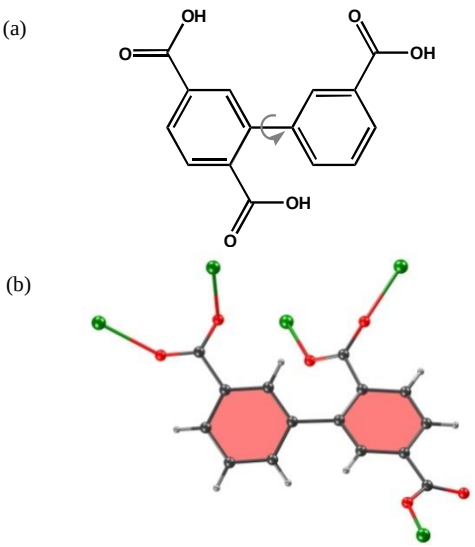

Fig. 1 biphenyl-3,2′,5′-tricarboxylic acid (H_3bptc) and its coordination modes in complexes **1**-**8**.

layer (Fig. 2d). The chelated phen ligands are arrayed along both sides of the layers, which are held together via π···π interactions between phenyl planes into a 3-D supramolecular network. The shortest distance between the two parallel phen planes is 3.5Å, which is within the common range for π···π interactions between the two phenyl rings.

From a topological viewpoint, an interesting structural feature in **1** is that the 2-D coordination layer can be rationalized as a binodal (3,6)-connected CdI_2-type network with a Schläfli symbol of $(4^3)_2(4^6{\cdot}6^6{\cdot}8^3)$. The CdI_2-type network with mixed nodes is one of the Catalan nets known in inorganic complexes such as metal alkoxides and hydroxides, [21] whereas only a few examples have been found in metal-organic coordination polymers.[22] As shown in Fig. 2e, the $bptc^{3-}$ ligand can be simplified as a 3-connected node (vertex symbol 4^3) and the Dy_2 dimer as a 6-connected node (vertex symbol $4^6{\cdot}6^6{\cdot}8^3$). Different from these reported networks, the 6-connected node adopts slightly distorted octahedral connecting mode and the 3-connected node adopts triangular pyramid mode resulting a distorted CdI_2-type network (Fig. 2e).

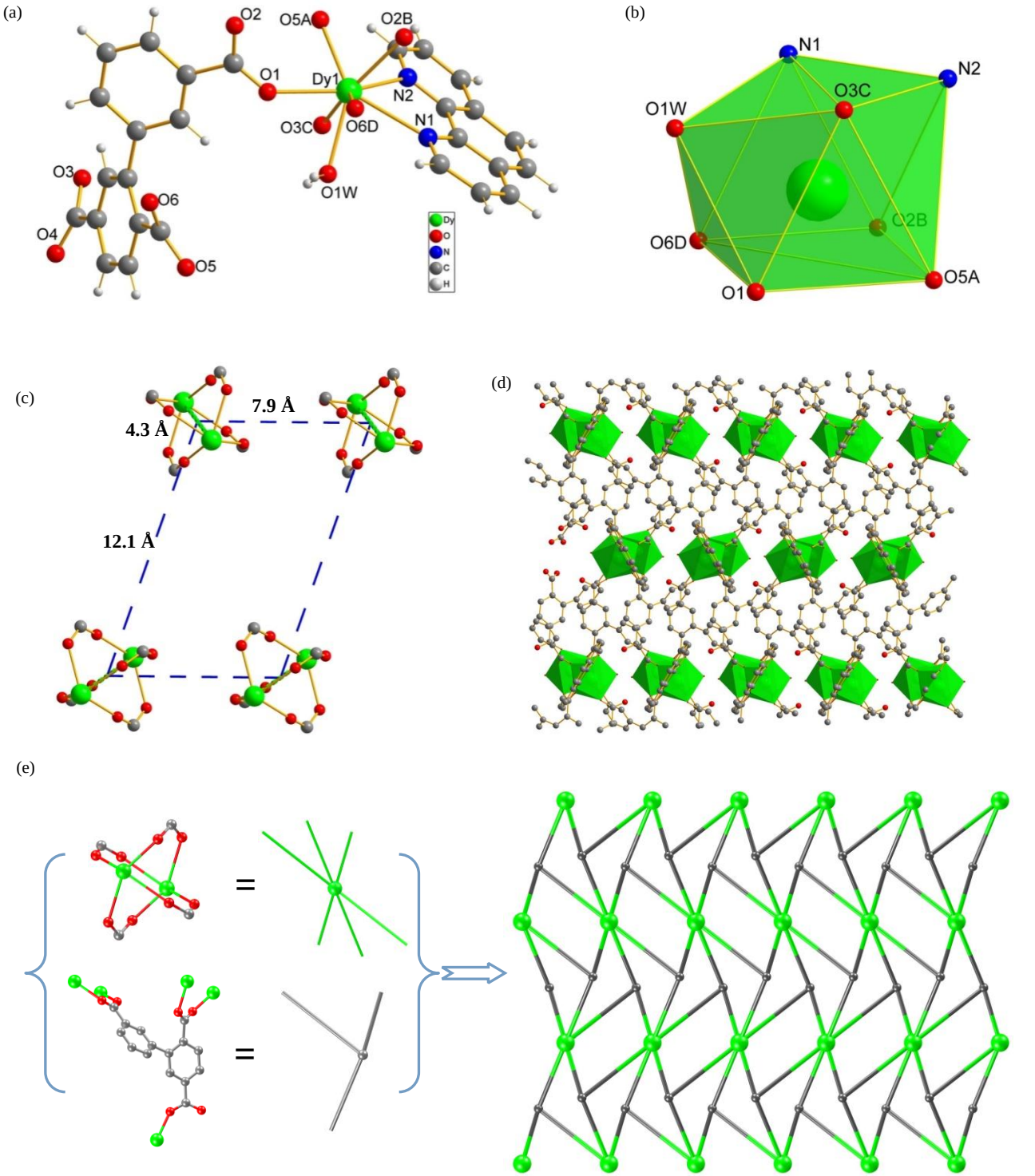

Fig. 2 (a) View of the coordination environments of Dy(III) atoms (A: x, y+1, z; B: -x+1/2, -y+1/2, -z; C: -x+1/2, y+1/2, -z+1/2; D: -x+1/2, -y-1/2, -z) and (b) polyhedron view of coordination geometry**;** (c) the distances of Dy···Dy in the dimer and Dy_2···Dy_2 between the adjacent dimers in the parallelogram unit**;** (d) polyhedron view of the 2D coordination layer viewed along the *c*-axis; (e) schematic view of the (6,3)-connected topology layer in **1**.

Thermal stability analysis

To examine the thermal stabilities of the eight complexes, we carried out the thermal gravimetric (TG) analyses (Fig. S2) and the measurement of the XRPD patterns to confirm the phase purity (Fig. S1). Samples of the complexes were heated to 700 °C under a nitrogen atmosphere. The results indicate that complexes **1–8** show similar thermal behavior owing to their isomorphous structures. Thus, only the thermal stabilities of complex **1** are discussed in detail (Fig. S2a). The TGA curve shows that the first weight loss of 2.7% from the beginning to 105 °C corresponds to the loss of the coordinated water molecule (calcd 2.8%) of one unit cell. Then the coordinated phen molecule began to be removed and were totally lost up to 530 °C (calculated: 28.0%, found: 28.2%), and then the structure was decomposed quickly before the final formation of metal oxide.

Magnetic property

Variable temperature magnetic susceptibility was measured for complex **1** in a 1 kOe dc field. At 300 K, the experimental $\chi_m T$ values is 27.1 $cm^3 \cdot mol^{-1} \cdot K$, which is consistent with the expected value (28.3 cm^3 mol^{-1} K) for two isolated Dy(III) ions ($^6H_{15/2}$, S=5/2, L=5, g=4/3) (Fig. 3a).[5a,23] When the temperature is lowered, the $\chi_m T$ value decreases gradually until about 100K, then more rapidly to a minimum value of 21.7 cm^3 mol^{-1} K at 1.8 K. Between 20 and 300 K, the magnetic susceptibilities can be fitted to the Curie–Weiss law with C_m = 27.8 $cm^3 \cdot mol^{-1} \cdot K$ and θ = -6.0 K (Fig. S3). This magnetic behavior suggests progressive depopulation of excited-state Stark sublevels due to the crystal-field effects of Dy(III) and/or antiferromagnetic interactions between the two Dy(III) ions in the dimer unit.[24] The magnetization increases rapidly at low field and eventually reaches the maximum value of 10.6 Nβ at 7 T without clear saturation, which is in relatively good agreement with the expected value (10.4 Nβ) for two isolated Dy(III) ions. The lack of saturation together with the non-superposition of the M versus HT^{-1} curves obtained at 2.0, 3.0 and 5.0 K suggests the large magneto-anisotropy and a low lying excited state present in this system.[25]

To investigate the magnetization dynamics, alternating current (ac) susceptibility measurements were carried out for **1**. The frequency-dependent increase in the in-phase signal and a concomitant appearance of an out-of-phase signal were observed in the absence of an external dc field (Fig. S3b), which indicates the onset of slow magnetization relaxation. However, no χ'' peaks due to the fast relaxation associated with the quantum tunneling of magnetization (QTM) at zero dc magnetic field can be observed even up to 1488 Hz, which can be ascribed to the degeneracy of the two ground Kramers states of each single dysprosium ion.[23,26]

For the purpose of better understanding the magnetic behavior of complex **1**, the ac susceptibility measurements were carried out under an external direct current (dc) magnetic field. Under an applied 1000 Oe magnetic field (Fig. 3b) , the ac susceptibility data show an overall reduction in height due to saturation effects that depress the susceptibility, and the observation of the clear χ_m'' peaks indicates an effective suppression of quantum tunneling relaxation of the magnetization (QTM).[27] The pre-exponential factor (τ_0) and energy barrier (U) to reverse the magnetization can be roughly estimated from the $\ln(\chi_m''/\chi_m')$ versus T^{-1} plots at a given frequency of the ac field by considering a single relaxation time (Fig. 3c). An effective energy barrier (and characteristic relaxation time) can be obtained by the least-squares fits of the experimental data through the expression $\chi_m''/\chi_m' = 2\pi\nu\tau_0 \exp(U/k_BT)$ giving $\tau_0 = 1.5 \times 10^{-7}$ s and U/k_B = 49.3 K at 99Hz, suggesting the presence of one thermally activated relaxation process under an external applied magnetic field.[28] Because of the fact that slow relaxation of magnetization is experimentally observed only over a short range of temperature, the estimation of these characteristic parameters might not be very accurate, but τ_0 is consistent with the expected numbers (τ_0 = 10^{-6} – 10^{-11} s) for SMMs.[29]

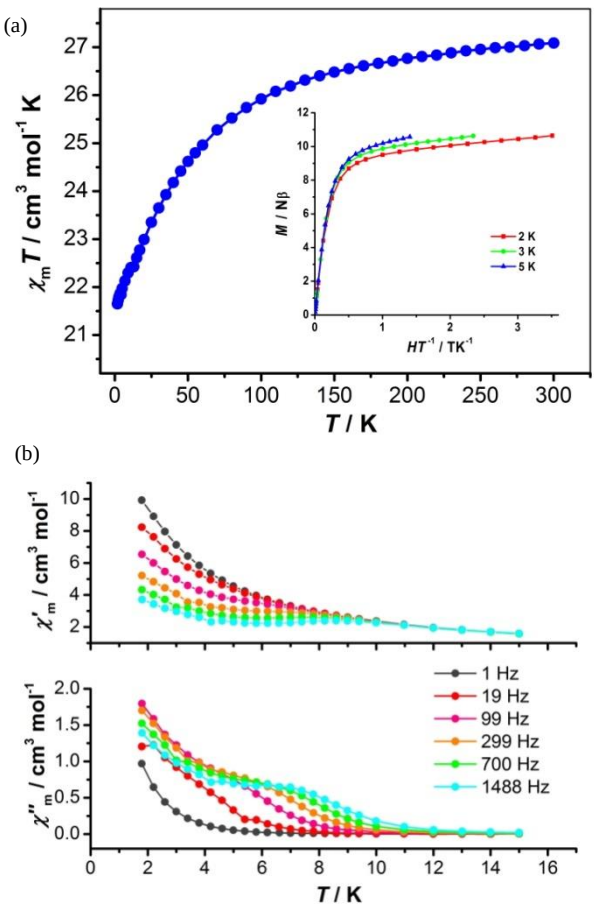

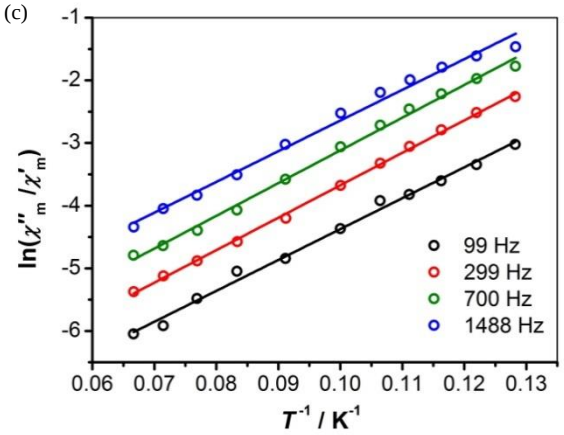

Fig. 3 (a) $\chi_m T$ versus T plots for **1** at an applied dc field of 1kOe (1.8-300K), the inset shows an M versus HT^{-1} plots at 2, 3, 5 K; (b) temperature-dependence of in-phase (χ') and out-of-phase (χ'') ac susceptibility signals (H_{dc} = 1000 Oe, H_{ac} = 5 Oe) at the indicated frequencies for **1**; (c) $\ln(\chi''/\chi')$ versus T^{-1} plots for **1** at different frequencies of the 5 Oe ac field (The solid lines are the best-fit curves).

In Eu(III) coordination polymers, the respective ground term of free Eu(III) ions ^{7}F state is split into seven states by spin-orbit coupling, and because of the weak energy separation, both the possible thermal population of the higher states and crystal field effects have influences on the magnetic properties.[30] As shown in Fig. 4, the χ_m value smoothly increases over the 300-100 K temperature range and then tends to a plateau. When the temperature is lowered from 30 K, χ_m values increase more rapidly, reaching a value of 0.02 cm^3·mol^{-1} at 1.8 K. At 300 K, the experimental $\chi_m T$ values is 3.1 cm^3·mol^{-1}·K, which is smaller than the theoretical high-temperature limit (4.5 cm^3·mol^{-1}·K) for two isolated Eu(III) ions (Fig. 4). The experimental $\chi_m T$ values decreases continuously because of the depopulation of Stack levels, reaching a value close to zero (0.03 cm^3·mol^{-1}·K) at 1.8 K, indicating that the f electrons of the Eu(III) ions depopulate from their magnetic excited states and populate the diamagnetic ground state of ^{7}F$_0$ during the cooling process.[30]

Though the Eu···Eu distance is 4.3 Å in the dimers, the superexchange interactions between the ions are very weak for the 4f electron structure. Compared to the Eu(III) mononuclear complexes, their curves of χ_m and $\chi_m T$ are very similar (Fig. 4).[31] Thus, the magnetic susceptibilities of **2** can be fitted with a single-ion Eu(III) model based on equation (**1**),[30c,d,31a] which only considers the spin-orbital coupling of Eu(III) ions.

$$\chi_m = \frac{A}{B}\cdot\frac{N\beta^2}{3kTx} + TIP \qquad (1)$$

$$A = 24 + \left(\frac{27x}{2} - \frac{3}{2}\right)\cdot e^{-x} + \left(\frac{135x}{2} - \frac{5}{2}\right)\cdot e^{-3x} + \left(189x - \frac{7}{2}\right)\cdot e^{-6x}$$

$$+\left(405x - \frac{9}{2}\right)\cdot e^{-10x} + \left(\frac{1458x}{2} - \frac{11}{2}\right)\cdot e^{-15x} + \left(\frac{2457x}{2} + \frac{13}{2}\right)\cdot e^{-21x}$$

$$B = 1 + 3e^{-x} + 5e^{-3x} + 7e^{-6x} + 9e^{-10x} + 11e^{-15x} + 13e^{-21x}$$

$$x = \frac{\lambda}{kT}$$

where λ being the spin-orbital coupling parameter, k being the Boltzmann constant and TIP being the temperature independent magnetism. By fitting the $\chi_m T$ versus T plots of the whole temperature range (Fig. 4), the best fitting results are λ = 326 cm^{-1} and $TIP = 5.98\times10^{-4}$ with an agreement factor R of 2.05×10^{-5} ($R = \sum[(\chi_m T)_{calcd}-(\chi_m T)_{obsd}]^2/\sum(\chi_m T)^2_{obsd}$). The λ value being the energy gap between the ^{7}F$_1$ and ^{7}F$_0$ free-ion states is comparable with that of the mononuclear Eu(III) complex (λ = 362 cm^{-1}) and other reported Eu(III) complexes.[30,31] The different values could originated from the different crystal field effect and/or site symmetry. The analyses for magnetic behaviors of **2** demonstrate that the Eu(III) ions are well isolated from each other in the magnetic molecule field, even if the Eu···Eu distance is rather short.[31]

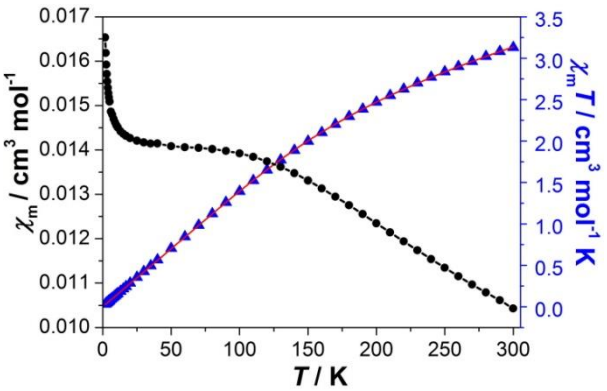

Fig. 4 χ_m versus T (black) and $\chi_m T$ versus T (blue) plots for **2** at an applied dc field of 1kOe (1.8-300K) (The red solid line is the best-fit curve).

For complex **3**, the experimental $\chi_m T$ values is 24.1 cm^3·mol^{-1}·K at 300 K, consistent with the expected value (23.6 cm^3 mol^{-1} K) for two isolated Tb(III) ions (^{6}H$_7$, S=3, L=3, g=3/2) (Fig. 5).[23] When the temperature is lowered, the $\chi_m T$ value decreases gradually until about 50K, then more rapidly to a minimum value of 12.86 cm^3·mol^{-1}·K at 1.8 K. Between 30 and 300 K, the magnetic susceptibilities can be fitted to the Curie–Weiss law with C_m = 24.4 cm^3·mol^{-1}·K and θ = -3.7 K (Fig. S4). The magnetization increases rapidly at low field and eventually reaches the maximum value of 9.8 Nβ at 7 T without clear saturation, which is much lower than the expected values for non-interacting Tb(III) ions.[32] The lack of saturation together with the non-superposition of the M versus HT^{-1} curves obtained at 2.0, 3.0 and 5.0 K suggests the presence of magneto-anisotropy and significant crystal field effects.[25,32] As no out-of-phase signal is observed in the ac magnetic susceptibility, there is no evidence of slow-relaxation for **3** down to 1.8 K.

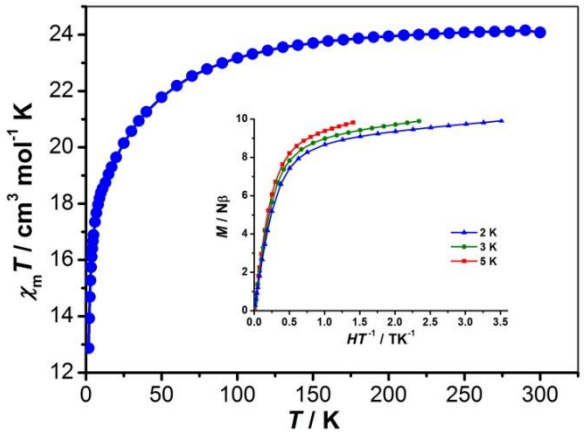

Fig. 5 $\chi_m T$ versus T plots for **3** at an applied dc field of 1kOe (1.8-300K), the inset shows an M versus HT^{-1} plots at 2, 3, 5 K

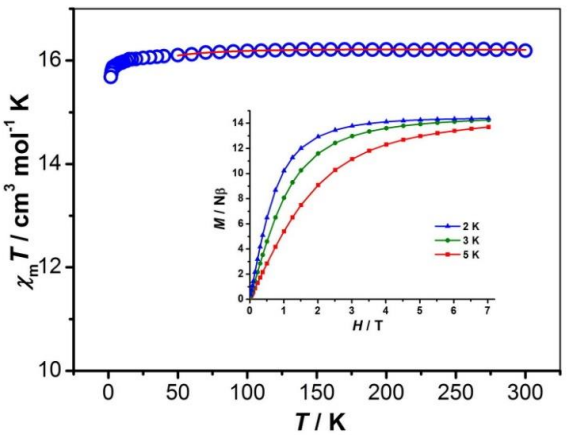

Fig. 6 $\chi_m T$ versus T plots for **4** at an applied dc field of 1kOe (1.8-300K) (The red solid lines are the best-fit curve), the inset shows an M versus H plots at 2, 3, 5 K.

For complex **4**, the experimental $\chi_m T$ values is 16.2 cm^3·mol^{-1}·K, close to the expected value (15.8 cm^3·mol^{-1}·K) for two isolated Gd(III) ions ($^8S_{7/2}$, S=7/2, g=2) (Fig. 6). When the temperature is lowered, the $\chi_m T$ value remains practically constant until about 30 K, then decreases rapidly to a minimum value of 15.7 cm^3·mol^{-1}·K at 1.8 K. Between 25 and 300 K, the magnetic susceptibilities can be fitted to the Curie–Weiss law with C_m = 16.7 cm^3·mol^{-1}·K and θ = -0.3 K (Fig. S5a).

Considering the structure based on binuclear Gd_2 units, the magnetic behavior can be interpreted with a binuclear model based on an isotropic spin Hamiltonian of $\hat{H} = -2JS_1S_2$ ($S_1 = S_2 = 7/2$), and the experimental data were analyzed using equation (**2**).[33]

$$\chi_m = \frac{2Ng^2\beta^2}{kT}\cdot\frac{A}{B} \qquad (2)$$

$$A = e^x + 5e^{3x} + 14e^{6x} + 30e^{10x} + 55e^{15x} + 140e^{28x}$$

$$B = 1 + 3e^x + 5e^{3x} + 7e^{6x} + 9e^{10x} + 11e^{15x} + 13e^{21x} + 15e^{28x}$$

$$x = \frac{J}{kT}$$

The best fit was obtained with a values of J = −0.041 cm^{-1}, and g = 2.03 with the agreement factor R of 5.57×10^{-5} ($R = \sum[(\chi_m T)_{calcd}-(\chi_m T)_{obsd}]^2/\sum(\chi_m T)^2_{obsd}$), indicating that weak antiferromagnetic coupling interactions exist between the adjacent Gd(III) ions in the dimer. The magnetization data of **4** are carried out at a field 0 − 7 T at 2.0, 3.0 and 5.0 K (Fig. 6). The magnetization exhibits a steady increase with increasing H and reach the expected saturation value of 14.0 Nβ for two individual Gd(III) ions. The large magnetization values and significant temperature dependency indicate that the complex may be promising candidates for cryogenic magnetic refrigeration.[34]

Luminescent property

Lanthanide coordination polymers show strong and characteristic luminescent emissions in the visible region upon excitation of ultraviolet radiation, making them good candidate for luminescent materials.[35] The luminescence spectra of complexes **1**-**3**, **5**-**7** were investigated in the solid-state at room temperature and exhibit clear characteristic emission spectra of the corresponding Dy(III), Eu(III), Tb(III), Sm(III) ions as shown in Fig. 7 and Fig. S6, except the Nd(III). According to our latest study, the free H_3bptc ligand displays strong emission around 484 nm upon excitation at 296 nm in solid state at room temperature, and the phen ligand displays strong emission around 390 nm attributed to the π* → π or π* → n transition (intraligand fluorescence).[17a] As shown in Fig. S6, the excitation spectra of **1**-**3**, **5** and **7** are similar to each other. All of them exhibit a wide band from 280 to 350 nm with two split peak around 296 and 330 nm, corresponding to the excitation peak of H_3bptc and phen ligand. Under excitation at 331 nm, the spectrum of **1** shows characteristic narrow emission bands at 479, 574, 662, 751 nm corresponding to the $^4F_{9/2} \rightarrow {}^6H_J$ (J = 15/2, 13/2, 11/2, 9/2) transitions. The most intensive emission at 574 nm belongs to the transition $^4F_{9/2} \rightarrow {}^6H_{13/2}$ of the Dy(III) ion. The emission at 479 nm is assigned to the transition $^4F_{9/2} \rightarrow {}^6H_{15/2}$, and the weaker emissions at 662 and 751 nm are attributed to the $^4F_{9/2} \rightarrow {}^6H_{11/2}$ and $^4F_{9/2} \rightarrow {}^6H_{9/2}$ transition in the complex.[36] Notably, the spectrum of **1** shows a broad and weak emission band centered around 386 nm, which can be attributed to the phen ligand-based emission. As shown in Fig. 4b, sharp emission lines from Eu(III) are observed originating from $^5D_0$ to ^7F_J (J = 1, 2, 3, 4) transitions.[36] The weaker emission at 592 nm ($^5D_0 \rightarrow {}^7F_1$) is due to the prominent magnetic dipole transition, which is almost unaffected by the coordination environment. The much stronger $^5D_0 \rightarrow {}^7F_2$ transition at 613 nm than the $^5D_0 \rightarrow {}^7F_1$ transition at 597 nm indicates the absence of inversion symmetry at the Eu(III) ion, which is in agreement with the results of the single crystal X-ray analysis. No emission from higher excited states (such as $^5D_1$) is observed, due to cross relaxation processes.[36a] Among the

emission lines, the $^5D_0 \rightarrow {}^7F_2$ transitions are the most striking, giving the intense red luminescence of complex **2**. As shown in Fig. 4c, the spectrum of **3** exhibits the characteristic emission bands for Tb(III) ion centered at 489, 544, 586 and 621 nm, which result from deactivation of the $^5D_4$ excited state to the corresponding ground state ^7F_J (J = 6, 5, 4, 3). The most intense emission is centered at 544 nm and corresponds to the hypersensitive transition $^5D_4 \rightarrow {}^7F_5$.[37] As shown in Fig. 4d, the spectrum of **5** exhibits four sharp bands at 561, 597, 643 and 705 nm characteristic of Sm(III), due to the transitions from the $^4G_{5/2}$ excited state to ^6H_J (J = 5/2, 7/2, 9/2, 11/2).[36a,c] The luminescent property of complex **6** was also determined, unfortunately it did not show characteristic emission bands of the Nd(III) ion in the near-IR region, which may be ascribed to the "quenching effect" of the aqua ligands.[38] The emission spectrum of 7 exhibits strong near-IR emission around 1008 nm, which can be assigned to the $^2F_{5/2} \rightarrow {}^2F_{7/2}$ transition of Yb(III) ion (Fig. 7e). Notably, the emission of the Yb(III) ion is not a single sharp transition, but appears another weaker band centered at 977 nm. The observed splitting may be attributed to the crystal field or stark splitting.[39] Different from complex **6**, even though the present Yb(III) complex contains the water molecule directly coordinated to lanthanide ions, the near-IR emission is still moderately intense.

It should be pointed out that the luminescent spectra of complexes **2**, **3**, **5** and **7** exhibit emission bands characteristic of the corresponding lanthanide ions, whereas the emissions arising from the free ligands are not observable (Fig. 7). The absence of ligand-based emission suggests energy can be effectively transferred from the ligands to the lanthanide center during the luminescent process. Comparably, the emission arising from the phen ligand observed in the spectra of **1** indicates the incomplete energy transfer from phen to the Dy(III) ions.[36,37]

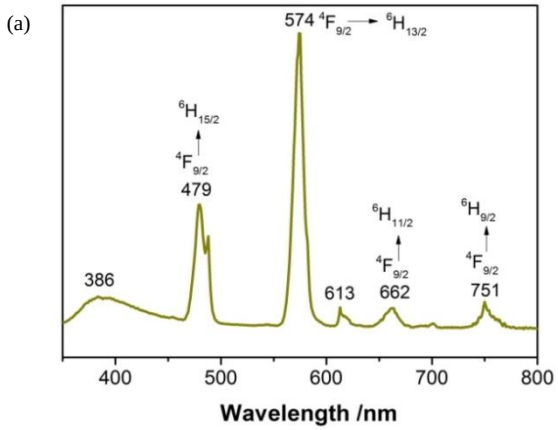

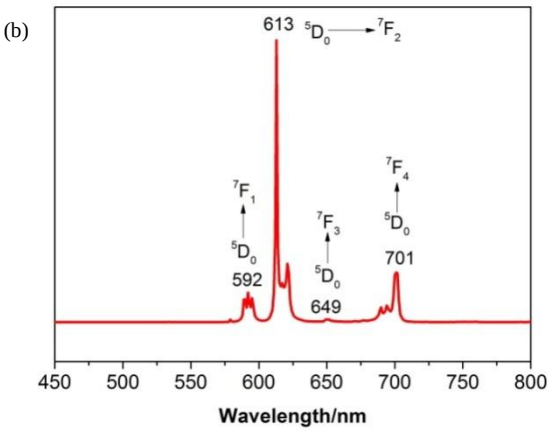

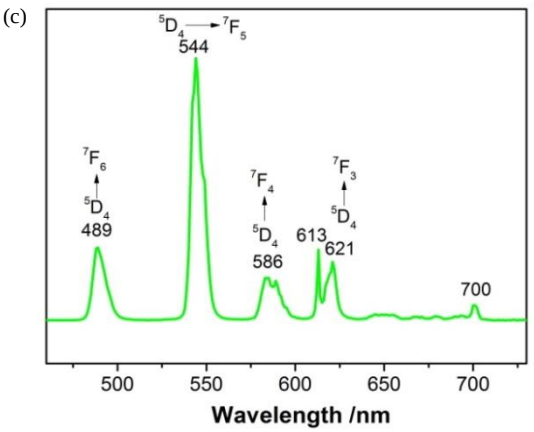

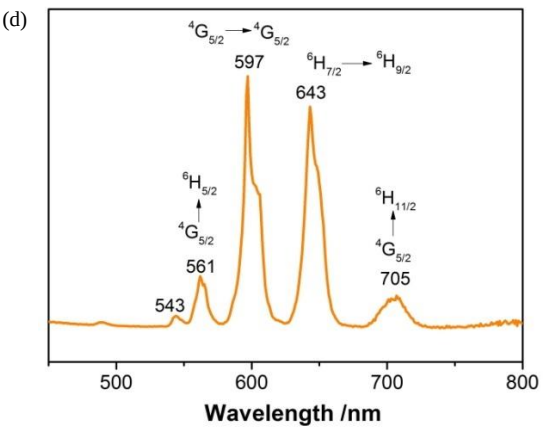

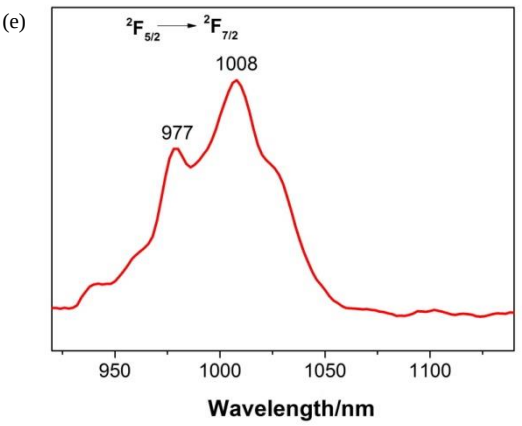

Fig. 7 (a) The emission spectra for complexes **1**(a), **2**(b), **3**(c), **5**(d) and **7**(e) in solid state at room temperature.

Conclusions

Eight isostructural lanthanide-organic coordination polymers involving asymmetric ligand with rotatable coordination vertex have been successfully synthesized and characterized. These complexes show (3,6)-connected CdI_2-type coordination network consisting of paddle-wheel dimers $[Ln_2(CO_2)_4]$. The asymmetric H_3bptc ligand has been fully deprotonated and has a dihedral angle of 47.5° between two phenyl rings, due to the coordination interactions to lanthanide ions. Magnetic studies show that Dy(III)-based complex **1** exhibits slow magnetization relaxation behaviour with frequency-dependent out-of-phase signals. Luminescent property studies reveal that five complexes exhibit emission bands characteristic of the corresponding lanthanide ions without the emissions arising from the free H_3bptc ligand, suggesting the ligand is capable of converting energy efficiently to the lanthanide centers.

Acknowledgements

This work was supported by the NSF of Guangdong Province (No. 2014A030313529), Science Foundation for The Excellent Youth Scholars in Higher Education Institutions of Guangdong Province (No. Yq201405), the Yang-cheng Scholars Foundation of Guangzhou (No. 12A002D) and Students' Innovation and Entrepreneurship Training Program (No. 201411078036 and 201311078025).

Notes and references

[a] *Guangzhou Key Laboratory for Environmentally Functional Materials and Technology, School of Chemistry and Chemical Engineering, Guangzhou University, Guangzhou 510006, P. R. China. Fax: 86 02039366908; Tel: 86 02039366908; E-mail: wangjgzhu@163.com*
[b] *Key Laboratory of Synthetic Bioinorganic Chemistry of Ministry of Education, School of Chemistry and Chemical Engineering, Sun Yat-Sen University, Guangzhou 510275, P. R. China*

† Electronic Supplementary Information (ESI) available: Crystallographic data in CIF format for **1**-**8**, XRPD patterns for **1**-**8**, TG curves for **1**-**8**, magnetic signals for **1**-**4**, excitation spectra for **1**-**3**, **5** and **7** selected bond lengths and angles for **1**-**8**. See DOI: 10.1039/b000000x/

1 (a) V. S. Sastri, J.-C.G. Bünzli, V. R. Rao, G. V. S. Rayudu and J. R. Perumareddi. *Modern Aspects of Rare Earths and Complexes*, Elsevier Science B.V., Amsterdam (2003); (b) C. Huang. *Rare Earth Coordination Chemistry, Fundamentals and Applications*, John Wiley & Sons (Asia), Singapore (2010).

2 (a) E. G. Moore, A. P. S. Samuel and K. N. Raymond, *Acc. Chem. Res.*, 2009, **42**, 542; (b) J.-C. G. Bünzli, *Chem. Rev.*, 2010, **110**, 2729; (c) D. N. Woodruff, R. E. P. Winpenny and R. A. Layfield, *Chem. Rev.*, 2013, **113**, 5110; (d) J.-C. G. Bünzli, *J. Coord. Chem.*, 2014, **67**, 3706; (e) J.-L. Liu, Y.-C. Chen, F.-S. Guo and M.-L. Tong, *Coord. Chem. Rev.*, 2014, **281**, 26.

3 (a) N. Sabbatini, M. Guardigli and J. M. Lehn, *Coord. Chem. Rev.* 1993, **123**, 20; (b) K. Binnemans, *Chem. Rev.*, 2009, **109**, 4283; (c) E. G. Moore, A. P. S. Samuel and K. N. Raymond, *Acc. Chem. Res.*, 2009, **42**, 542.; (d) Y.-J. Cui, Y.-F. Yue, G.-D. Qiang and B.-L. Chen, *Chem. Rev.*, 2012, **112**, 1126.

4 (a) B. D. Chandler, D. T. Cramb and G. K. H. Shimizu, *J. Am. Chem. Soc.*, 2006, **128**, 10403; (b) P. Mahata, K. V. Ramya and S. Natarajan, *Chem.-Eur. J.*, 2008, **14**, 5839; (c) S. V. Eliseeva, D. N. Pleshkov, K. A. Lyssenko, L. S. Lepnev, J.-C. G. Bünzli and N. P. Kuzmina, *Inorg. Chem.*, 2010, **49**, 9300; (d) J. Xu, W. Su and M. Hong, *Cryst. Growth Des.*, 2011, **11**, 337.

5 (a) C. Benelli and D. Gatteschi, *Chem. Rev.*, 2002, **102**, 2369; (b) D. Gatteschi, R. Sessoli and J. Villain, *Molecular Nanomagnets*, Oxford University Press: Oxford, 2006.

6 (a) P. Zhang, Y. N. Guo and J. Tang, *Coord. Chem. Rev.*, 2013, **257**, 1728; (b) N. F. Chilton, D. Collison, E. J. L. McInnes, R. E. P. Winpenny and A. Soncini, *Nat. Commun.*, 2013, **4**, 2551; (c) P.-H. Guo, J.-L. Liu, J.-H. Jia, J. Wang, F.-S. Guo, Y.-C. Chen, W.-Q. Lin, J.-D. Leng, D.-H. Bao, X.-D. Zhang, J.-H. Luo and M.-L. Tong, *Chem. Eur. J.*, 2013, **19**, 8769; (d) P.-H. Guo, J.-L. Liu, Z.-M. Zhang, L. Ungur, L. F. Chibotaru, J.-D. Leng, F.-S. Guo and M.-L. Tong, *Inorg. Chem.*, 2012, **51**, 1233; (e) Y. Meng, J.-L. Liu, Z.-M. Zhang, Q.-W. Li, Z.-J. Lin and M.-L. Tong, *Dalton Trans.*, 2013, **42**, 12853; (f) P.-H. Guo, Y. Meng, Y.-C. Chen, Q.-W. Li, B.-Y. Wang, J.-D. Leng, D.-H. Bao, J.-H. Jia and M.-L. Tong, *J. Mater. Chem. C*, 2014, **2**, 8858; (g) J.-L. Liu, Y.-C. Chen, Y.-Z. Zheng, W.-Q. Lin, L. Ungur, W. Wernsdorfer, L. F. Chibotaru and M.-L. Tong, *Chem. Sci.*, 2013, **4**, 3310; (h) J.-L. Liu, J.-Y. Wu, Y.-C. Chen, V. Mereacre, A. K. Powell, L. Ungur, L. F. Chibotaru, X.-M. Chen and M.-L. Tong, *Angew. Chem., Int. Ed.*, 2014, **53**, 12966.

7 (a) J. D. Rinehart and J. R. Long, *Chem. Sci.*, 2011, **2**, 2078; (b) L. Sorace, C. Benelli and D. Gatteschi, *Chem. Soc. Rev.*, 2011, **40**, 3092; (c) D. N. Woodruff, R. E. P. Winpenny and R. A. Layfield, *Chem. Rev.*, 2013, **113**, 5110; (c) F. Habib and M. Murugesu, *Chem. Soc. Rev.*, 2013, **42**, 3278; (d) R. J. Blagg, L. Ungur, F. Tuna, J. Speak, P. Comar, D. Collison, W. Wernsdorfer, E. J. L. McInnes, L. F. Chibotaru and R. E. P. Winpenny, *Nat. Chem.*, 2013, **5**, 673; (d) Y. Z. Zheng, G. J. Zhou, Z. P. Zheng and R. E. P. Winpenny, *Chem. Soc. Rev.*, 2014, **43**, 1462.

8 (a) Z. R. Herm, J. A. Swisher, B. Smit, R. Krishnai and J. R. Long, *J. Am. Chem. Soc.*, 2011, **133**, 5664; (b) T. M. McDonald, W. R. Lee, J. A. Mason, B. M. Wiers, C. S. Hong and J. R. Long, *J. Am. Chem. Soc.*, 2012, **134**, 7056; (c) X. J. Li, F. L. Jiang, M. Y. Wu, S. Q. Zhang, Y. F. Zhou and M. C. Hong, *Inorg. Chem.*, 2012, **51**, 4116; (d) X. Feng, X.–L. Ling, L. Liu, H.-L. Song, L.-Y. Wang, S. W. Ng and B.-Y. Su, *Dalton Trans.*, 2013, **42**, 10292; (e) L.-M. Fan, X.-T. Zhang, W. Zhang, Y.-S. Ding, W.-L. Fan, L.-M. Sun, Y. Pang and X. Zhao, *Dalton Trans.*, 2014, **43**, 6701.

9 (a) L. J. Murray, M. Dinca, J. Yano, S. Chavan, S. Bordiga, C. M. Brown and J. R. Long, *J. Am. Chem. Soc.*, 2010, **132**, 7856; (b) L. Luo, G.-C. Lv, P. Wang, Q. Liu, K. Chen and W.-Y. Sun, *CrystEngComm*, 2013, **15**, 9537; (c) X. Zhang, Y.-Y. Huang, Q.-P. Lin, J. Zhang and Y.-G. Yao, *Dalton Trans.*, 2013, **42**, 2294; (d) Y.-W. Li, J.-R. Li, L.-F. Wang, B.-Y. Zhou, Q. Chen and X.-H. Bu, *J. Mater. Chem. A*, 2013, **1**, 495.

10 (a) W.-J. Ji, Q.-G. Zhai, S.-N. Li, Y.-C. Jiang and M.-C. Hu, *Chem. Commun.*, 2011, **47**, 3834; (b) P. Song, B. Liu, Y.-Q. Li, J.-Z. Yang, Z.-M. Wang and X.-G. Li, *CrystEngComm*, 2012, **14**, 2296; (c) G.-H. Cui, C.-H. He, C.-H. Jiao, J.-C. Geng and V. A. Blatov, *CrystEngComm*, 2012, **14**, 4210; (d) E. Yang, Q.-R. Ding, Y. Kang and F. Wang, *Inorg. Chem. Commun.*, 2013, **36**, 195.

11 (a) J. Wang, Z.-J. Lin, Y.-C. Ou, N.-L. Yang, Y.-H. Zhang and M.-L. Tong, *Inorg. Chem.*, 2008, **47**, 190; (b) X.-Y. Wang and S. C. Sevov, *Inorg. Chem.*, 2008, **47**, 1037; (c) J. Wang, S.-H. Yang, A.-J. Zhou, Z.-Q. Liu and J. Zhao, *J. Coord. Chem.*, 2013, **66**, 2413.

12 (a) E .Yang, J. Zhang, Z.-J. Li, S. Gao, Y. Kang, Y.-B. Chen, Y.-H. Wen and Y.-G. Yao, *Inorg. Chem.*, 2004, **43**, 6525; (b) S. M. Humphrey, R. A. Mole, R. I. Thompson and P. T. Wood , *Inorg. Chem.*, 2010, **49**, 3441.

13 (a) R.-Q. Zhong, R.-Q. Zou, M. Du, T. Yamada, G. Maruta, S. Takeda, J. Li and Q. Xu, *CrystEngComm*, 2010, **12**, 677; (b) S. A. Sapchenko, D. N. Dybtsev, D. G. Samsonenko and V. P. Fedin, *New J. Chem.*, 2010, **34**, 2445; (c) G.-P. Zhou, Y.-L. Yang, R.-Q. Fan, W.-W. Cao and B. Yang, *CrystEngComm*, 2012, **14**, 193; (d) P. K. Yadav, N. Kumari, P. Pachfule, R. Banerjee and L. Mishra, *Cryst. Growth Des.*, 2012, **12**, 5311; (e) F. Guo, F. Wang, Hui Yang, X.-L. Zhang and J. Zhang, *Inorg. Chem.*, 2012, **51**, 9677.

14 (a) Z.-Y. Guo, H. Xu, S.-Q. Su, J.-F. Cai, S. Dang, S.-C. Xiang, G.-D. Qian, H.-J Zhang, M. O. Keeffed and B.-L. Chen, *Chem. Commun.*, 2011, **47**, 5551; (b) Z.-J. Zhang, L.-P. Zhang, L. Wojtas, P. Nugent,

M. Eddaoudi and M. J. Zaworotko, *J. Am. Chem. Soc.*, 2012, **134**, 924; (c) C.-C. Ji, J. Li, Y.-Z. Li, Z.-J. Guo and H.-G. Zheng, *CrystEngComm*, 2011, **13**, 459; (d) L.-N. Li, S.-Y. Wang, T.-L. Chen, Z.-H. Sun, J.-H. Luo and M.-C. Hong, *Cryst. Growth Des.*, 2012, **12**, 4109.

15 (a) Q.-P. Lin, T. Wu, S.-T. Zheng, X.-H. Bu and P.-Y. Feng, *Chem. Commun.*, 2011, **47**, 11852; (b) J. Jia, M. Shao, T.-T. Jia, S.-R. Zhu, Y.-M. Zhao, F.-F. Xing and M.-X. Li, *CrystEngComm*, 2010, **12**, 1548; (c) I. A. Ibarra, S.-H. Yang, X. Lin, A. J. Blake, P. J. Rizkallah, H. Nowell, D. R. Allan, N. R. Champness, P. Hubberstey and M. Schröder, *Chem. Commun.*, 2011, **47**, 8304; (d) X.-T. Zhang, L.-M. Fan, Z. Sun, W. Zhang, D.-C. Li, J.-M. Dou and L. Han, *Cryst. Growth Des.*, 2013, **13**, 792; (e) J. Zhao, D.-S. Li, X.-J. Ke, B. Liu, K. Zou and H.-M. Hu, *Dalton Trans.*, 2012, **41**, 2560; (f) S.-H. Yang, J.-L. Sun, A. J. Ramirez-Cuesta, S. K. Callear, W. I. F. David, D. P. Andersonl, R. Newby, A. J. Blake, J. E. Parker, C. C. Tang and M. Schröder, *Nat. Chem.*, 2012, **4**, 887.

16 (a) M.-L. Cao, J.-J. Wu, J.-J. Liang and B.-H. Ye, *Cryst. Growth Des.*, 2010, **10**, 4934; (b) G.-F. Zi, F.-R. Zhang, L. Xiang, Y. Chen, W.-H. Fang and H.-B. Song, *Dalton Trans.*, 2010, **39**, 4048; (c) H.-L. Wang, D.-P. Zhang, D.-F. Sun, Y.-T Chen, K. Wang, Z.-H. Ni, L.-J. Tian and J.-Z. Jiang, *CrystEngComm*, 2010, **12**, 1096; (d) S.-Q. Su, W. Chen, C. Qin, S.-Y. Song, Z.-Y. Guo, G.-H. Li, X.-Z Song, M. Zhu, S. Wang, Z.-M. Hao and H.-J. Zhang, *Cryst. Growth Des.*, 2012, **12**, 1808; (e) H.-L. Hsiao, C.-J. Wu, W. Hsu, C.-W. Yeh, M.-Y. Xie, W.-J. Huang and J.-D. Chen, *CrystEngComm*, 2012, **14**, 8143; (f) Z.-J. Lin, and M.-L. Tong, *Coord. Chem. Rev.*, 2011, **255**, 421.

17 (a) J. Zhao, L.-Q. Xie, Y.-M. Ma, A.-J. Zhou, W. Dong, J. Wang, Y.-C. Chen and M.-L. Tong, *CrystEngComm*, 2014, **16**, 10006; (b) B. Liu, B. Liu, L.-Y. Pang, G.-P. Yang, L. Cui, Y.-Y. Wang and Q.-Z. Shi, *CrystEngComm*, 2013, **15**, 5205; (c) Z.-Q. Gao, H.-J. Li, M. K. Alexander, J.-Z. Gu, *Chinese J. Struct. Chem.*, 2014, **33**, 888.

18 G. M. Sheldrick, *SHELXTL97*, program for cystal structure refinement, University of Göttingen, Germany, 1997.

19 (a) J. Wang, Y.-H. Zhang and M.-L. Tong. *Chem. Commun.*, 2006, 3166; (b) J. Wang, S. Hu and M.-L. Tong. *Eur. J. Inorg. Chem.*, 2006, 2069; (c) J. Wang, Z.-J. Lin, Y.-C. Ou, Y. Shen, R. Herchel and M.-L. Tong. *Chem. Eur. J.*, 2008, **24**, 7218; (d) J. Wang, Y.-C. Ou, Y. Shen, L. Yun, J.-D. Leng, Z.-J. Lin and M.-L. Tong, *Cryst. Growth Des.*, 2009, **9**, 2442.

20 (a) J. Yang, S.-Y. Song, J.-F. Ma, Y.-Y. Liu and Z.-T. Yu, *Cryst. Growth Des.*, 2011, **11,** 5469; (b) L. Liang, G. Peng, G.-Z. Li, Y.-H. Lan, A. K. Powell and H. Deng, *Dalton Trans.*, 2012, **41**, 5816; (c) Y.-M. Song, F. Luo, M.-B. Luo, Z.-W. Liao, G.-M. Sun, X.-Z. Tian, Y. Zhu, Z.-J. Yuan, S.-J. Liu, W.-Y. Xu and X.-F. Feng, *Chem. Commun.*, 2012, **48**, 1006; (d) F. Pointillart, B. L. Guennic, S. Golhen, O. Cador and L. Ouahab, *Chem. Commun.*, 2013, **49**, 11632.

21 (a) C. G. Subhash, A. M. Michael, Y. C. Michael and E. B. William, *J. Am. Chem. Soc.*, 1991, **113**, 1884; (b) D. Thomas, E. Michel, M. L. Yves and C. Enric, *J. Am. Chem. Soc.*, 2003, **125**, 3295.

22 (a) N. Snejko, C. Cascales, B. Gomez-Lor, E. Guti_errez-Puebla, M. Iglesias, C. Ruiz-Valero and M.A. Monge, *Chem. Commun.*, 2002, 1366; (b) B. Yan, C. S. Day and A. Lachgar, *Chem. Commun.*, 2004, 2390; (c) G.-H. Wang, Y.-Q. Lei, N. Wang, R.-L. He, H.-Q. Jia, N.-H. Hu and J.-W. Xu, *Cryst. Growth Des.*, 2010, **10**, 534; (d) Z.-B. Han, G.-X. Zhang, M.-H. Zeng, D.-Q. Yuan, Q.-R. Fang, J.-R. Li, J. Rivas and H.-C. Zhou, *Inorg. Chem.* 2010, **49**, 769; (e) X.-T. Zhang, L.-M. Fan, X. Zhao, D. Sun, D.-C. Li and J.-M. Dou, *CrystEngComm*, 2012, **14**, 2053.

23 (a) J. P. Sutter and M. L. Kahn, *Magnetism*: *Molecules to Materials*, Vol. 5, Eds.: J. S. Miller and M. Drillon, Wiley VCH, Weiheim, **2005**, 161; (b) R. Sessoli and A. K. Powell, *Coord. Chem. Rev.*, 2009, **253**, 2328.

24 (a) J. Long, F. Habib, P.-H. Lin, I. Korobkov, G. Enright, L. Ungur, W. Wernsdorfer, L. F. Chibotaru and M. Murugesu, *J. Am. Chem. Soc.*, 2011**,** **133**, 5319; (b) S.-D. Jiang, B.-W. Wang, H.-L. Sun, Z.-M. Wang and S. Gao, *J. Am. Chem. Soc.*, 2011, **133**, 4730; (c) W.-Q. Lin, X.-F. Liao, J.-H. Jia, J.-D. Leng, J.-L. Liu, F.-S. Guo and M.-L. Tong, *Chem. Eur. J.*, 2013, **19**, 12254.

25 (a) P.-H. Lin, T. J. Burchell, L. Ungur, L. F. Chibotaru and W. Wensdorfer, *Angew. Chem., Int. Ed.*, 2009, **48**, 9489; (b) M. Ren, S.-S. Bao, N. Hoshino, T. Akutagawa, B. Wang, Y.-C. Ding, S. Wei and L.-M. Zheng, *Chem. Eur. J.*, 2013, **19**, 9619.

26 (a) S.-D. Jiang, B.-W. Wang, G. Su, Z.-M. Wang and S. Gao, *Angew. Chem., Int. Ed.*, 2010, **49**, 7448; (b) H. Wang, W. Cao, T. Liu, C. Duan and J. Jiang, *Chem. Eur. J.*, 2013, **19**, 2266; (c) W. Cao, Y.-H. Zhang, H.-L. Wang, K. Wang and J.-Z. Jiang, *RSC Adv.*, 2015, **5**, 17732.

27 (a) J. Bartolomé, G. Filoti, V. Kuncser, G. Schinteie, V. Mereacre, C. E. Anson, A. K. Powell, D. Prodius and C. Turta, *Phys. Rev. B*, 2009, **80**, 14430; (b) Y.-L. Miao, J.-L. Liu, J.-Y. Li, J.-D. Leng, Y.-C. Ou and M.-L. Tong, *Dalton Trans.*, 2011, **40**, 10229.

28 (a) H.-L. Wang, K. Wang, J. Tao and J.-Z. Jiang, *Chem. Commun.*, 2012, **48**, 2973; (b) W. Cao, Y.-H. Zhang, H.-L. Wang, K. Wang and J.-Z. Jiang, *RSC Adv.*, 2015, **5**, 17732.

29 (a) M. T. Gamer, Y. Lan, P. W. Roesky, A. K. Powell and R. Clérac, *Inorg. Chem.*, 2008, **47**, 6581; (b) Y. Gao, G. Xu, L. Zhao, J. Tang and Z. Liu, *Inorg. Chem.*, 2009, **48**, 11495; (c) D. N. Woodruff, R. E. P. Winpenny and R. A. Layfield, *Chem. Rev.*, 2013, **113**, 5110.

30 (a) M.-F. Wu, M.-S. Wang, S.-P. Guo, F.-K. Zheng, H.-F. Chen, X.-M. Jiang, G.-N. Liu, G.-C. Guo and J.-S. Huang, *Cryst. Growth Des.*, 2011, **11**, 372; (b) N. Xu, C. Wang, W. Shi, S.-P. Yan, P. Cheng and D.-Z. Liao, *Eur. J. Inorg. Chem.* **2011**, 2387; (c) L.-F. Wang, L.-C. Kang, W.-W. Zhang, F.-M. Wang, X.-M. Ren and Q.-J. Meng, *Dalton Trans.*, 2011, **40**, 9490; (d) X.-J. Wang, Z.-M. Cen, Q.-L. Ni, X.-F. Jiang, H.-C. Lian, L.-C. Gui, H.-H. Zuo and Z.-Y. Wang, *Cryst. Growth Des.*, 2010, **10**, 2960.

31 (a) M. Andruh, E. Bakalbassis, O. Kahn, J. C. Trombe and P. Porcher, *Inorg. Chem.*, 1993, **32**, 1616; (b) C.-M. Liu, M. Xiong, D.-Q. Zhang, M. Du and D.-B. Zhu, *Dalton Trans.*, 2009, 5666; (c) E. Chelebaeva, J. Larionova, Y. Guari, R. A. S. Ferreira, L. D. Carlos, F. A. Almeida Paz, A. Trifonov and C. Guérin, *Inorg. Chem.*, 2009, **48**, 5983.

32 (a) S.-W. Zhang, W. Shi, L.-L. Li, E.-Y. Duan and P. Cheng, *Inorg. Chem.*, 2014, **53**, 10340; (b) J.-M. Zhou, W. Shi, N. Xu and P. Cheng, *Cryst. Growth Des.*, 2013, **13**, 1218; (c) X.-Q. Zhao, X.-H. Liu, J.-J. Lia and B. Zhao, *CrystEngComm*, 2013, **15**, 3308.

33 (a) A. Panagiotopoulos, T. F. Zafiropoulos, S. P. Perlepes, E. Bakalbassis, I. Masson-Ramade, O. Kahn, A. Terzis and C. P. Raptopoulou, *Inorg. Chem.*, 1995, **34**, 4918; (b) A.-J. Zhang, Y.-W. Wang, W. Dou, M. Dong, Y.-L. Zhang, Y. Tang, W.-S. Liu and Y. Peng, *Dalton Trans.*, 2011, **40**, 2844; (c) S.-Q. Su, S. Wang, X.-Z. Song, S.-Y. Song, C. Qin, M. Zhu, Z.-M. Hao, S.-N. Zhao and H.-J. Zhang, *Dalton Trans.*, 2012, **41**, 4772; (d) B.-M. Ji, D.-S. Deng, X. He, B. Liu, S.-B. Miao, N. Ma, W.-Z. Wang, L.-G. Ji, P. Liu and X.-F. Li, *Inorg. Chem.* 2012, **51**, 2170.

34 (a) Y. Meng, Y.-C. Chen, Z.-M. Zhang, Z.-J. Lin and M.-L. Tong, *Inorg. Chem.*, 2014, **53**, 9052; (b) Y.-C. Chen, L. Qin, Z.-S. Meng, D.-F. Yang, C. Wu, Z.-D. Fu, Y.-Z. Zheng, J.-L. Liu, R. Tarasenko, M. Orendáč, J. Prokleška, V. Sechovsky´ and M.-L. Tong, *J. Mater. Chem. A*, 2014, **2**, 9851.

35 (a) G. Vicentini, L. B. Zinner, J. Zukerman-Schpector and K. Zinner, *Coord. Chem. Rev.*, 2000, **196**, 353; (b) R. Martínez-Máñez and F. Sancenón, *Chem. Rev.*, 2003, **103**, 4419; (c) W. M. Yen, S. Shionoya and H. Yamamoto, *Phosphor Handbook*, CRC Press, Athens, 2007.

36 (a) Y.-G. Sun, B. Jiang, T.-F. Cui, G. Xiong, P. F. Smet, F. Ding, E.-J. Gao, T.-Y. Lv, K. V. Eeckhout, D. Poelman and F. Verpoort, *Dalton Trans.*, 2011, **40**, 11581; (b) Q.-F. Yang, Y. Yu, T.-Y. Song, J.-H. Yu, X. Zhang, J.-Q. Xu, and T.-G. Wang, *CrystEngComm*, 2009, **11**, 1642; (c) Y.-H. Luo, F.-X. Yue, X.-Y. Yu, X. Chen and H. Zhang, *CrystEngComm*, 2013, **15**, 6340; (d) Y.-T. Liu, Y.-Q. Du, X. Wu, Z.-P. Zheng, X.-M. Lin, L.-C. Zhu and Y.-P. Cai, *CrystEngComm*, 2014, **16**, 6797.

37 (a) J. Yang, S.-Y. Song, J.-F. Ma, Y.-Y. Liu and Z.-T. Yu, *Cryst. Growth Des.*, 2011, **11**, 5469; (b) J.-Z. Gu, J. Wu, D.-Y. Lv, Y. Tang, K.-Y. Zhu and J.-C. Wu, *Dalton Trans.*, 2013, **42**, 4822; (c) D. Poelman, P. F. Smet, B.-Y. Rena and Y.-G. Sun, *Dalton Trans.*, 2014, **43**, 3462.

38 (a) Q.-F. Yang, Y. Yu, T.-Y. Song, J.-H. Yu, X. Zhang, J.-Q. Xu and T.-G. Wang, *CrystEngComm*, 2009, **11**, 1642; (b) L.-N. Jia, L. Hou, L. Wei, X.-J. Jing, B. Liu, Y.-Y. Wang and Q.-Z. Shi, *Cryst. Growth Des.*, 2013, **13**, 1570; (c) X. Feng, X.-L. Ling, L. Liu, H.-L. Song, L.-Y. Wang, S.-W. Ng and B.-Y. Su, *Dalton Trans.*, 2013, **42**, 10292.

39 (a) P. -F. Yan, S. Chen, P. Chen, J.-W. Zhang and G.-M. Li, CrystEngComm, 2011, 13, 36; (b) D. J. Lewis, F. Moretta, A. T. Holloway and Z. Pikramenou, Dalton Trans., 2012, 41, 13138; (c) W.-T. Xu, Y.-F. Zhou, D.-C. Huang, W. Xiong, M.-Y. Su, K. Wang, S. Han and M.-C. Hong, *Cryst. Growth Des.*, 2013, **13**, 5420; (d) Y.-L. Gai, K.-C. Xiong, L. Chen, Y. Bu, X.-J. Li, F.-L. Jiang and M.-C. Hong, *Inorg. Chem.*, 2012, **51**, 13128.